Figure S3.1: **Number of 256 bp haplotype paths in the graphs with an increasing number of variants added to the graphs.**
The line plot is fitted using loess function in R.
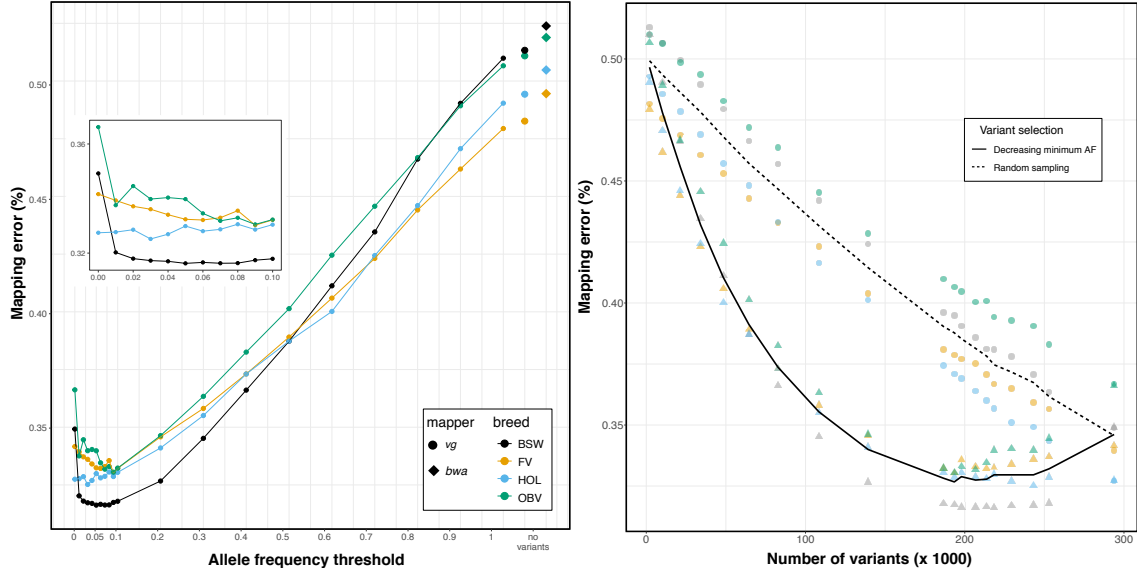
Figure S3.2: **Single-end mapping accuracy using genome graphs that contained variants filtered for allele frequency.**
(a) Proportion of incorrectly mapped reads for four breed-specific augmented genome graphs. Diamonds and large dots represent results from linear mapping using *BWA mem* and *vg*, respectively. The inset is a larger representation of the mapping accuracy for alternate allele frequency thresholds less than 0.1. (b) Read mapping accuracy for breed-specific augmented graphs that contained variants that were either filtered for alternate allele frequency (triangles) or sampled randomly (circles) from all variants detected within a breed. The dashed and solid line represents the average proportion of mapping errors across four breeds using variant prioritization and random sampling.
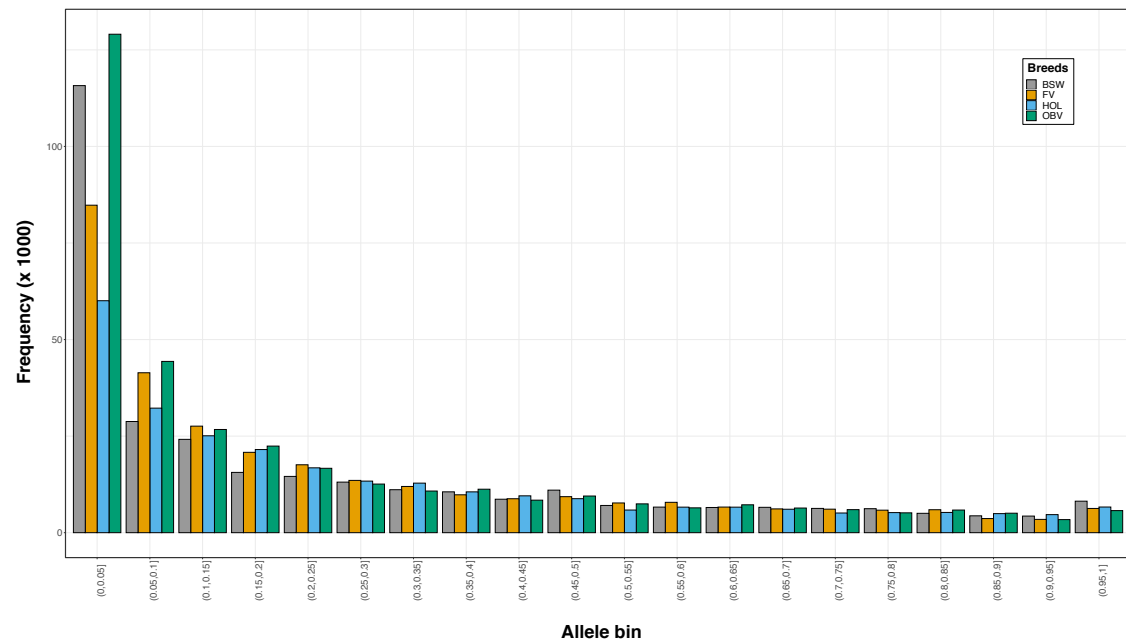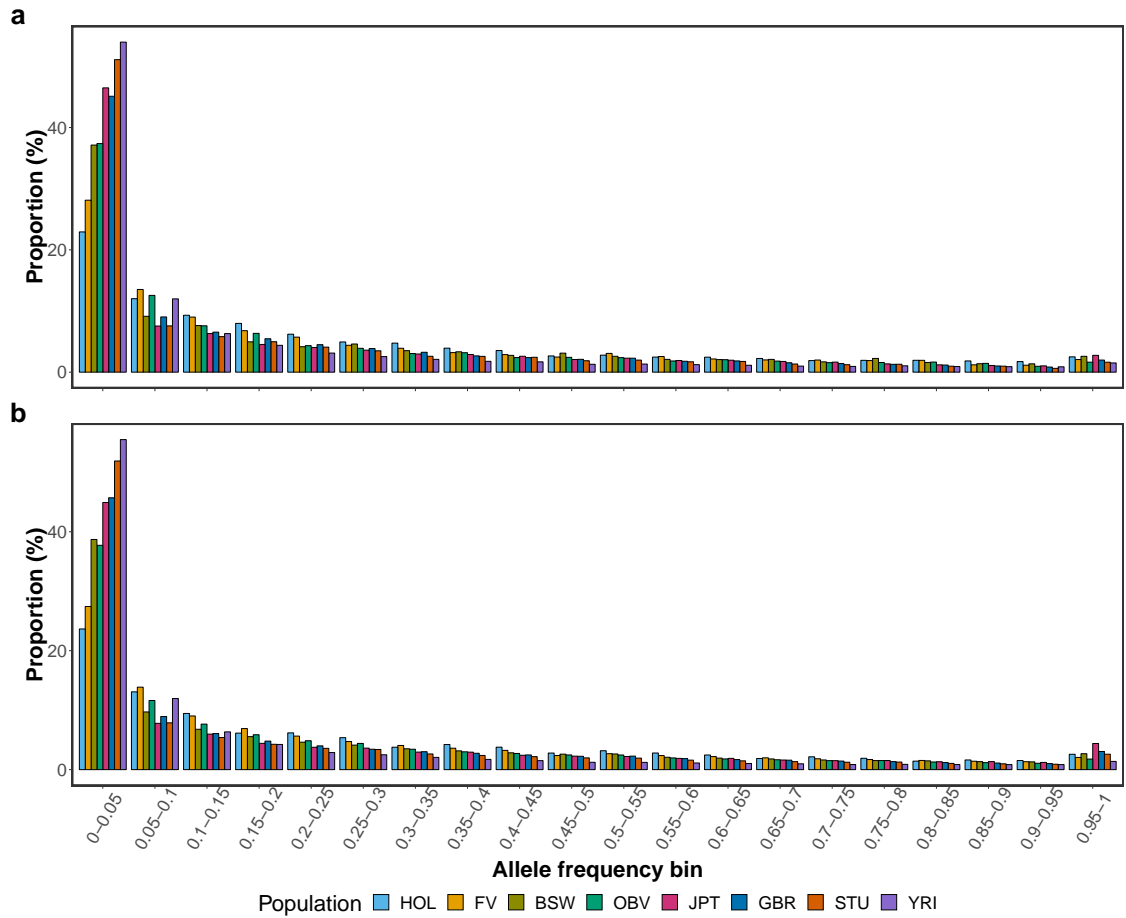
Figure S3.3: **Number of variants detected on chromosome 25 in 82 BSW, 49 FV, 49 HOL and 108 OBV cattle.**
Variants are binned according to allele frequency.

a

b

Figure S3.4: **Distribution of alternate allele frequencies in four cattle breeds and four human populations based on (a) bta25 and human chromosome 19 used for graph construction, and (b) whole genome variants.**
The bars indicate the proportion of sequence variants for 20 allele frequency classes. Different colour indicates cattle breeds (HOL, FV, BSW, OBV) and human populations (JPT, GBR, STU, YRI).
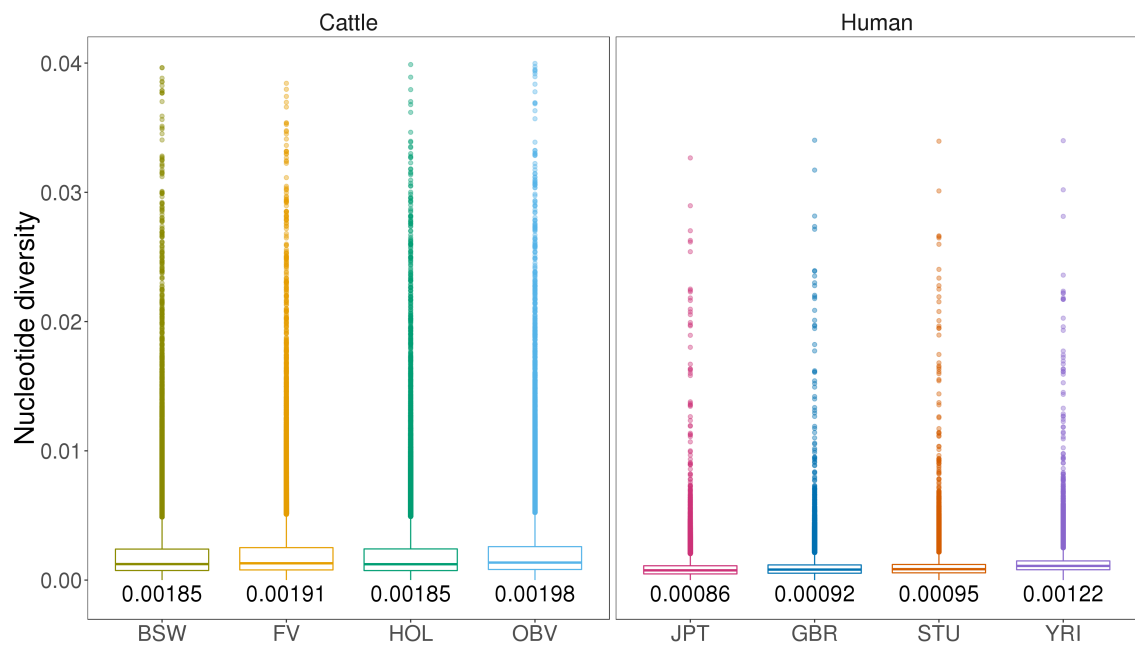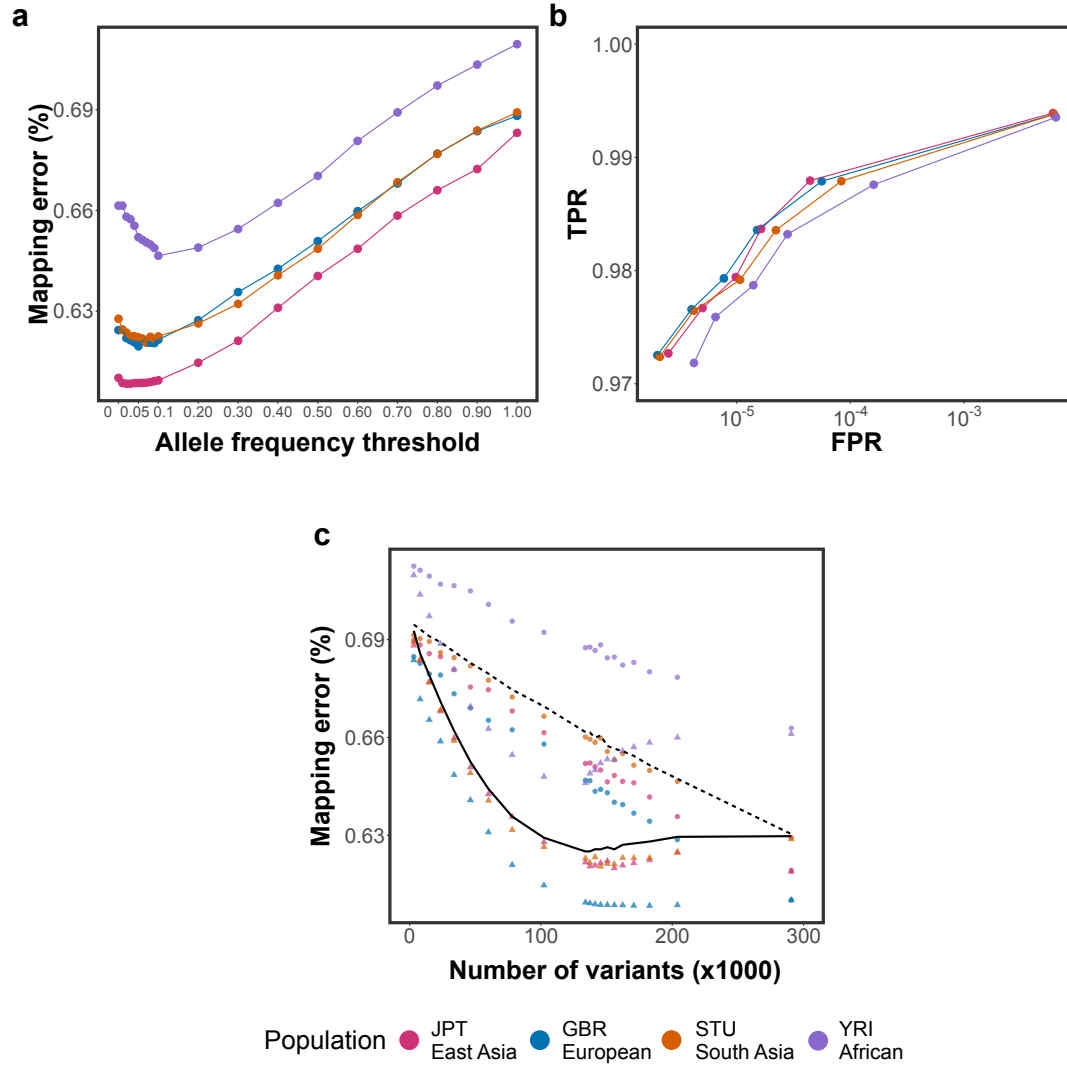
Figure S3.5: **Nucleotide diversity (π) based on whole genome autosomal variants in cattle and human.**
Nucleotide diversity (π) from each population calculated using vcftools with 10 kb non-overlapped windows based on whole genome autosomal variants. Number under the boxplot indicates average across windows.

Figure S3.6: **Single-end mapping accuracy using four human population-specific augmented graphs.**
(a) Proportion of incorrectly mapped reads for four populationspecific augmented genome graphs (b) True positive (sensitivity) and false positive mapping rate (specificity) parameterized based on the mapping quality for the best performing graph from each population. (c) Read mapping accuracy for population specific augmented graphs that contained variants that were either filtered for alternate allele frequency (triangles) or sampled randomly (circles) from all variants detected within a population. The dashed and solid line represents the average proportion of mapping errors across four populations using variant prioritization and random sampling.
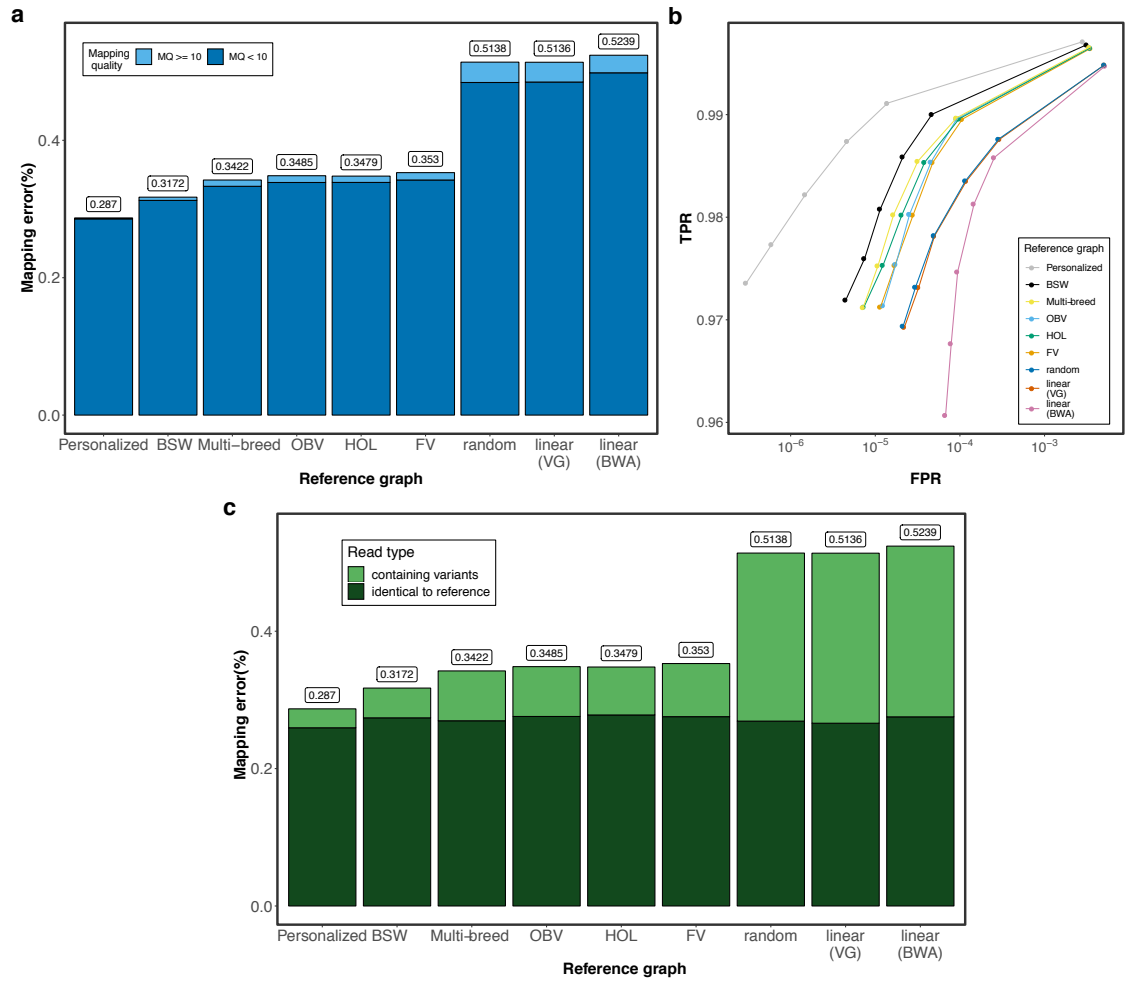
Figure S3.7: **The accuracy of mapping simulated BSW single-end reads to variation-aware and linear reference structures.**
(a) Proportion of BSW single-end reads that mapped erroneously against breed-specific augmented graphs, random graphs or linear reference sequences. Dark and light blue colours represent the proportion of incorrectly mapped reads with mapping quality (MQ)<10 and MQ>10, respectively. (b) True positive (sensitivity) and false positive mapping rate (specificity) parameterized based on the mapping quality. (c) Dark and light green colours represent the proportion of incorrectly mapped reads that matched corresponding reference nucleotides and contained non-reference alleles, respectively
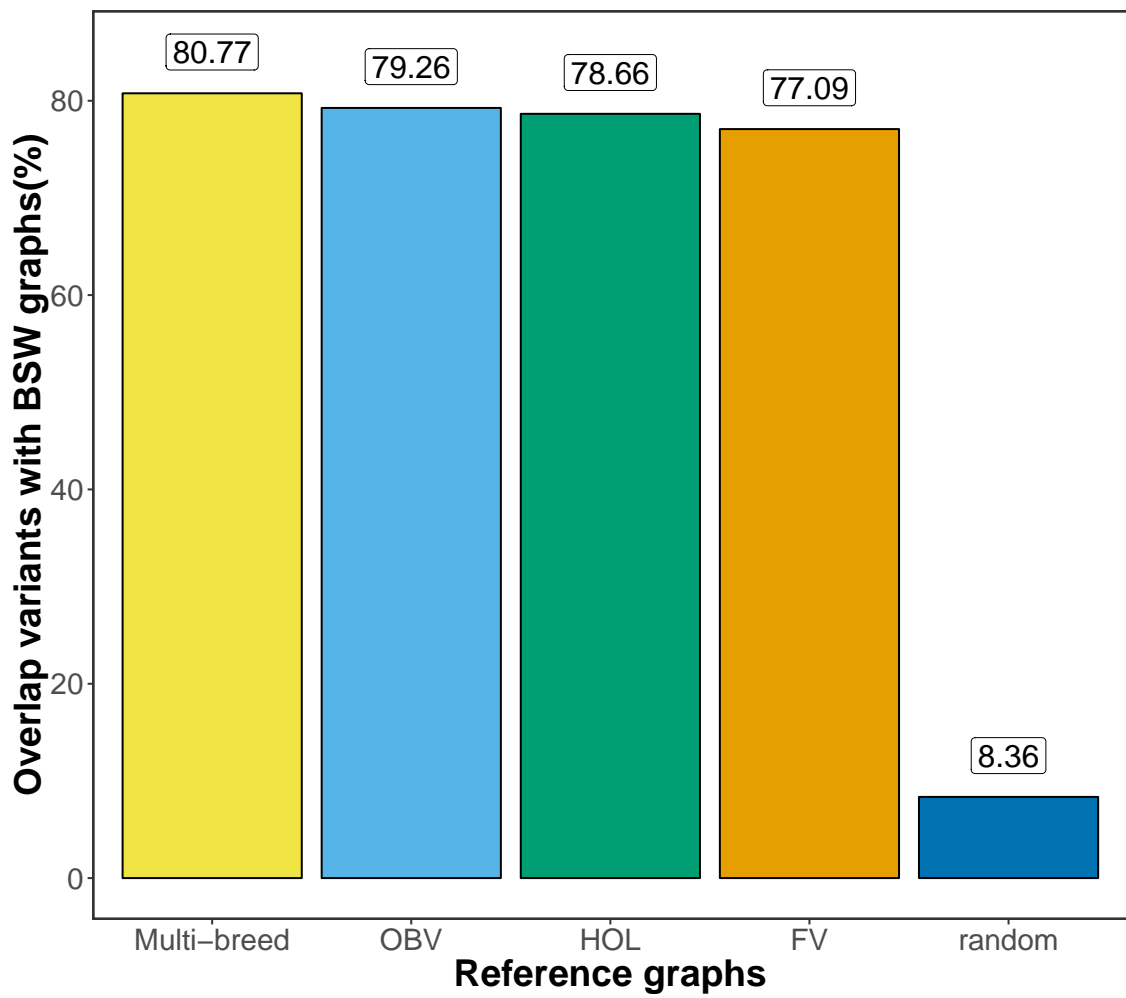
Figure S3.8: **Overlap of the variants**
(N=243,145) between the BSW-and all other variation-aware reference graphs. The values are averaged across 10 replicates.

a

	FV	HOL	OBV	Linear(BWA)	Multi-breed	Random	Linear(VG)
Random							0.35
Multi-breed						1.7e−70	5.8e−70
Linear(BWA)					4.3e−84	9.5e−53	1.2e−53
OBV				5.1e−83	0.00025	7.7e−69	2.6e−68
HOL			0.033	1.1e−83	0.35	6.7e−70	2.3e−69
FV		0.35	0.35	2.8e−83	0.0079	3e−69	9.9e−69
BSW	9.1e−30	2e−27	4e−31	5.7e−88	4.2e−25	2.8e−76	7.8e−76

b

	FV	HOL	OBV	Linear(BWA)	Multi-breed	Random	Linear(VG)
Random							0.74
Multi-breed						1.4e−119	1.4e−119
Linear(BWA)					2.6e−121	1.9e−33	8.3e−34
OBV				3e−120	2e−21	1.5e−118	1.6e−118
HOL			0.44	2.5e−120	2e−19	1.4e−118	1.4e−118
FV		5.4e−17	7e−15	1.7e−119	3.6e−35	9.9e−118	9.9e−118
BSW	6.7e−71	2.9e−66	8.9e−67	2.7e−125	5.4e−60	9.6e−124	9.8e−124

Figure S3.9: **Pairwise heatmap of *P-values* from *t tests***
comparing 8 graph-based mapping scenarios for (a) paired- and (b) single-end reads. The
P-values are adjusted for multiple testing using Bonferroni-correction.
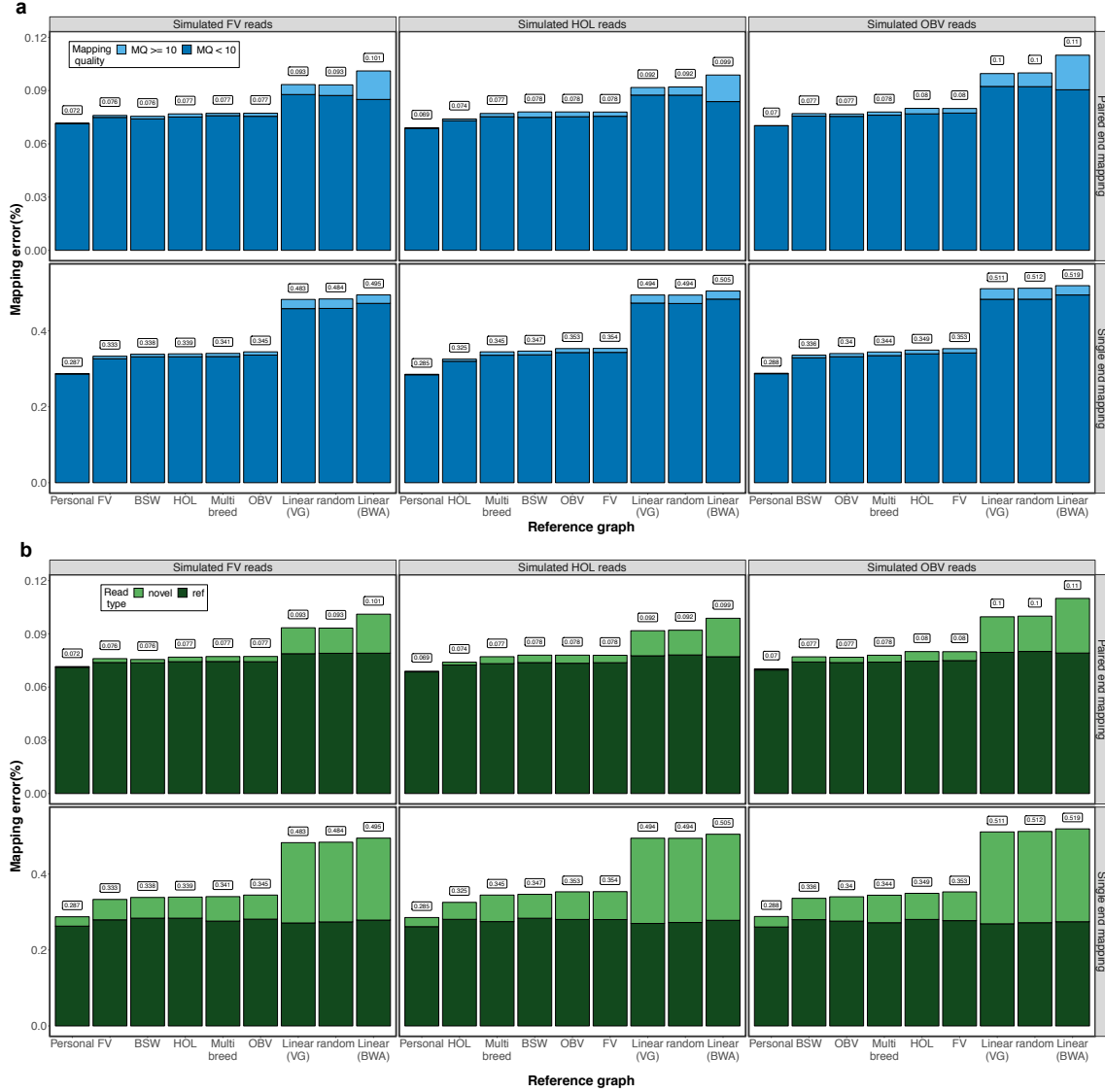
Figure S3.10: **The accuracy of mapping simulated FV, HOL and OBV reads to variation-aware and linear reference structures.**
(a) Proportion of reads that mapped erroneously against personalized graphs, breed-specific augmented graphs, random graphs or linear reference sequences. Dark and light blue colours represent the proportion of incorrectly mapped reads with mapping quality (MQ)<10 and MQ>10, respectively. The upper and lower panels reflect paired-end and single-end reads, respectively. (b) Dark and light green colours represent the proportion of incorrectly mapped reads that matched corresponding reference nucleotides and contained non-reference alleles, respectively. The upper and lower panels reflect paired-end and single-end reads, respectively
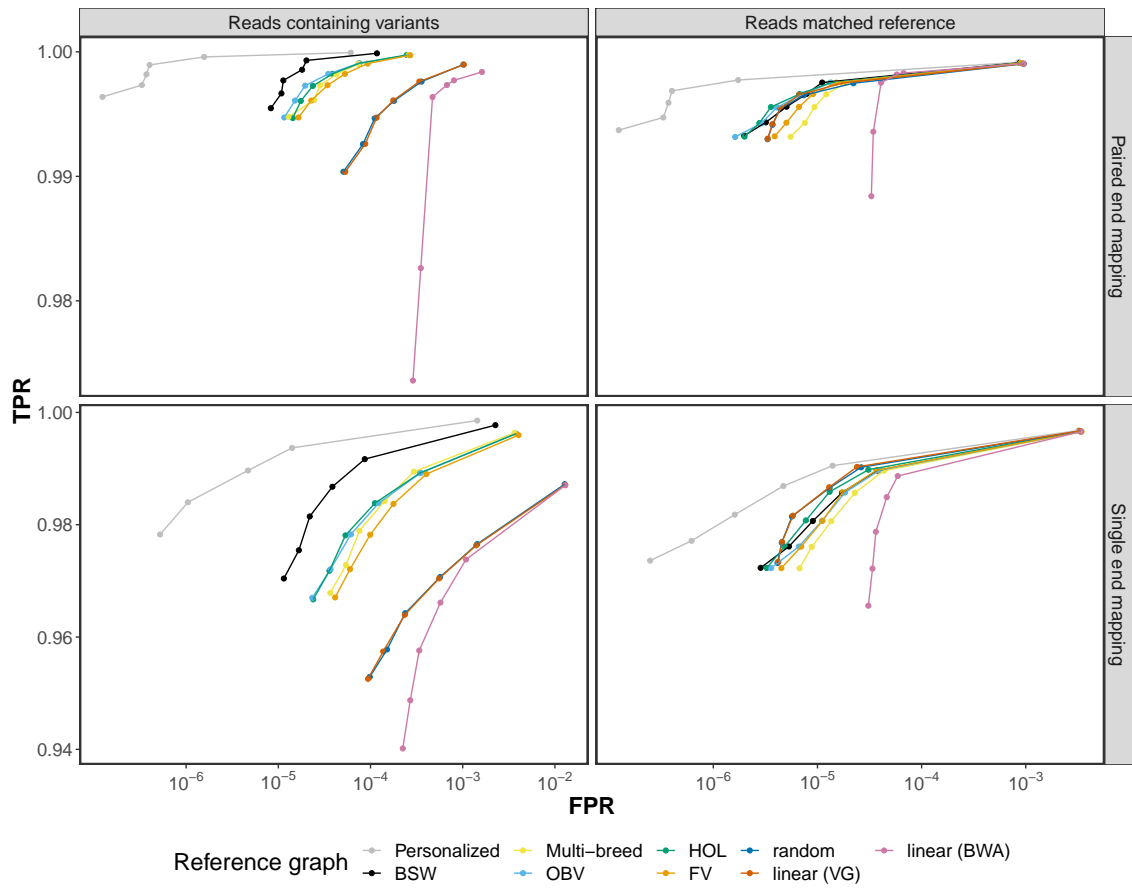
Figure S3.11: **ROC curves split by read's novelty**
Cumulative *True positive* and *False positive rate* at different mapping quality thresholds visualized as Receiver Operating Characteristic (ROC) curves for reads than contain variants and match corresponding reference alleles. The upper and lower panels represent results from paired- and single-end reads.
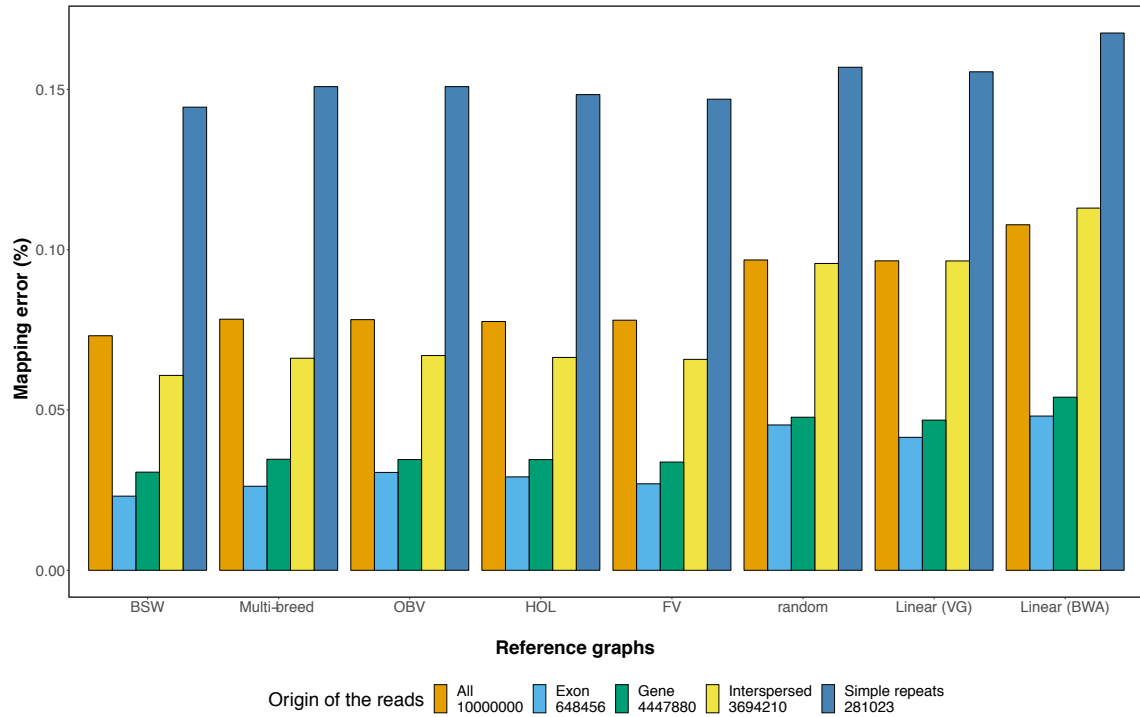
Figure S3.12: **Mapping accuracy for reads originating from different genomic features.**
The origin of 10 million simulated reads was determined based on the Bos taurus ARS-UCD1.2 ensembl 99 annotations (exonic and genic) and the ARS-UCD1.2 repeat regions labelled by Repeat Masker (Interspersed duplications including SINEs, LINEs, LTR, and DNA transposable elements, and simple repeats which contain low-complexity and simple repetitive regions). Different colour indicates the proportion of erroneously mapped reads for each annotation category. The orange bars represent the average proportion of mis-mapped reads for six graph-based (BSW, Multi-breed, OBV, HOL, FV, random) and two linear (VG, BWA) reference structures. Reads were simulated from haplotypes of a BSW individual.
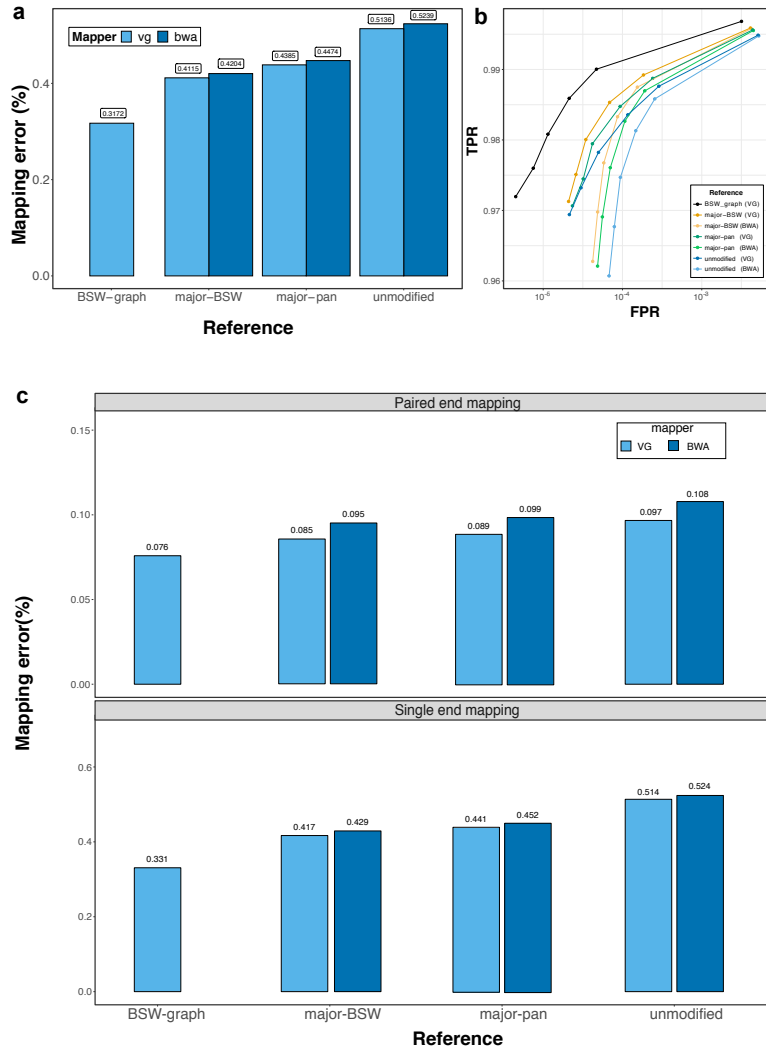
Figure S3.13: **Single-end read mapping accuracy using breed-specific augmented genome graphs and consensus linear reference sequences.**
(a) Dark and light blue represent the proportion of reads that mapped incorrectly using *BWA mem* and *vg*, respectively, to the BSW-specific augmented reference graph (BSW-graph), the BSW-specific (major-BSW) and multi-breed linear consensus sequence (major-pan) and the bovine linear reference sequence (unmodified). (b) True positive (sensitivity) and false positive mapping rate (specificity) parameterized based on the mapping quality. (c) Paired- and single-end read mapping accuracy using breed-specific augmented genome graphs and consensus linear reference sequences that were only adjusted at SNPs.
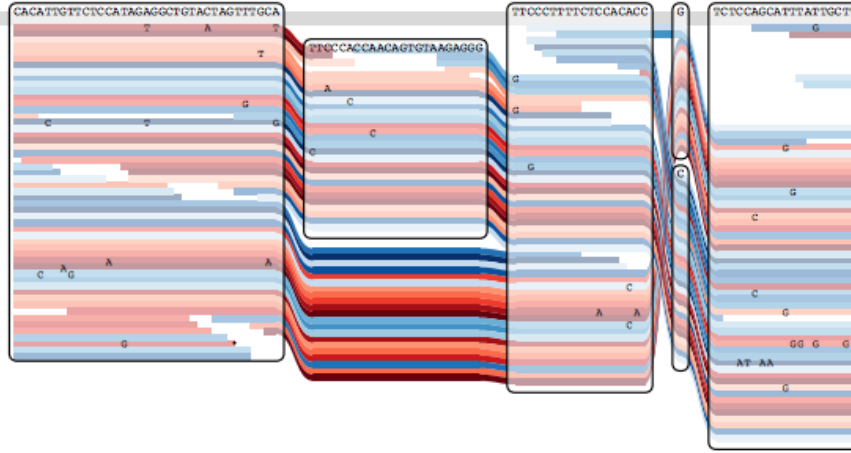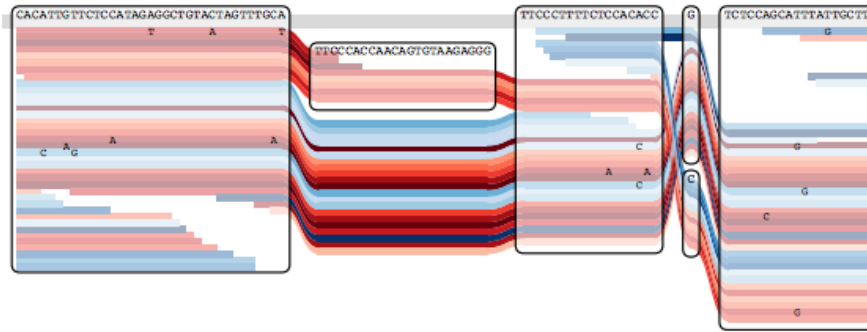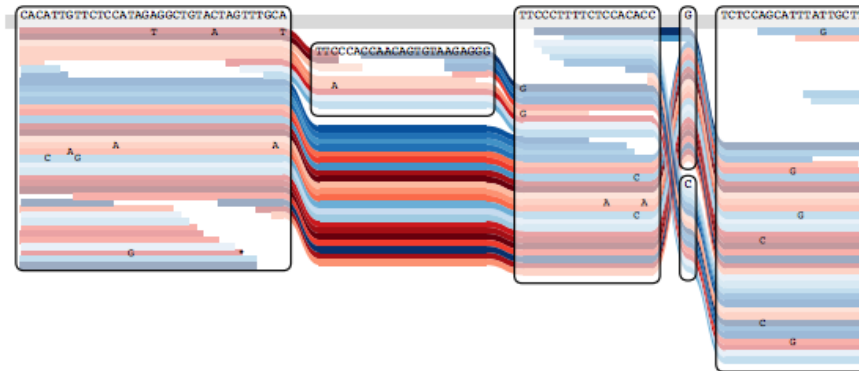
Figure S3.14: **Graph alignment visualization.**
Visualization of a 23-bp insertion at Chr10: 5,941,270 in graph and linear alignments using the *sequence tube map* tool (Beyer et al., 2019). The variant was called heterozygous from the linear alignment, but the allelic ratio was highly biased towards the reference allele. Visual inspection suggests that more reads supporting the alternate allele are present in the graph alignments. Red and blue colour indicates forward and reverse reads, respectively. The reads from the linear alignment were realigned to the variation-aware graph for the purpose of the visualisation.
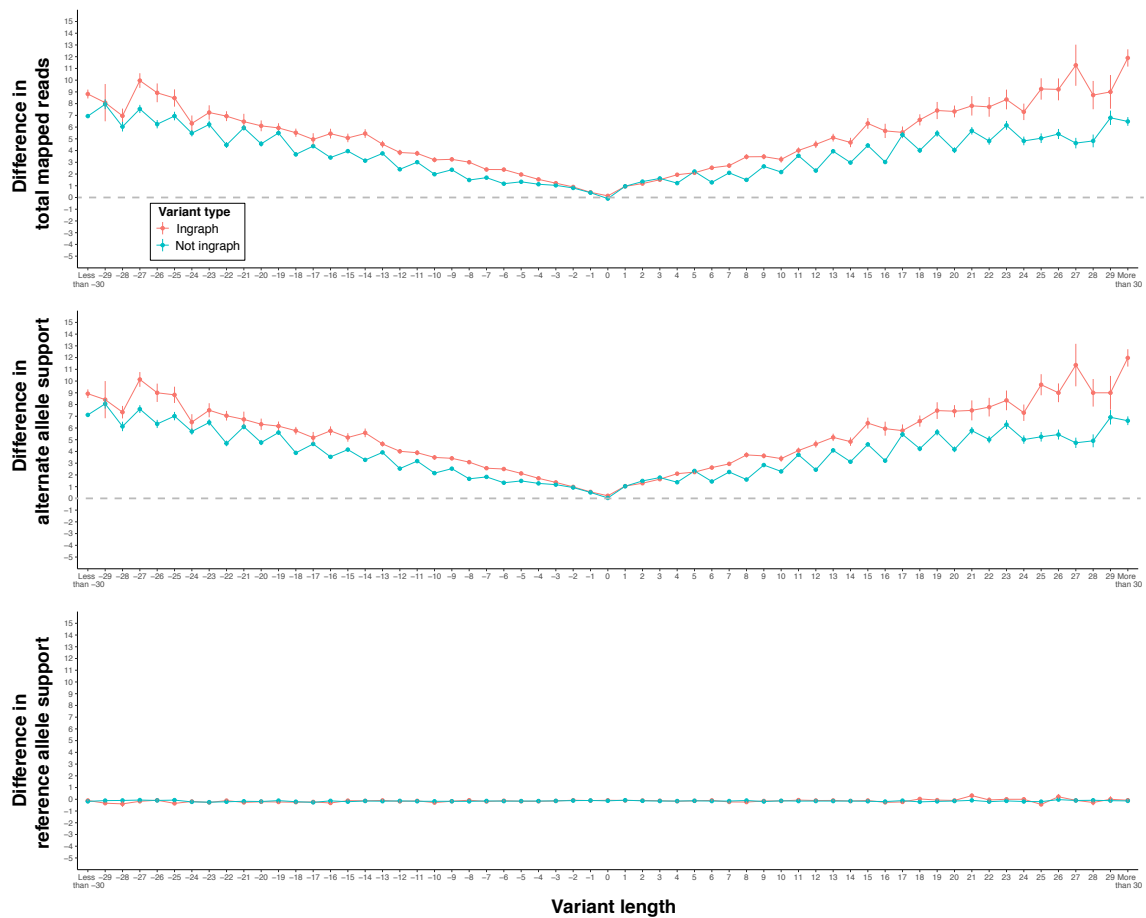
Figure S3.15: **Difference in the total of mapped reads, and reads support for reference and alternate alleles** between the graph-based and BWA alignments for deletions, SNPs and insertions. Positive values indicate a larger number of reads for graph-based alignments. The dashed grey line indicates equal support for graphbased and linear alignments. The circles represent the mean (± standard error of mean) values at a given variant length. Red and green colour indicates that the alternate allele is included and not included in the graph, respectively.
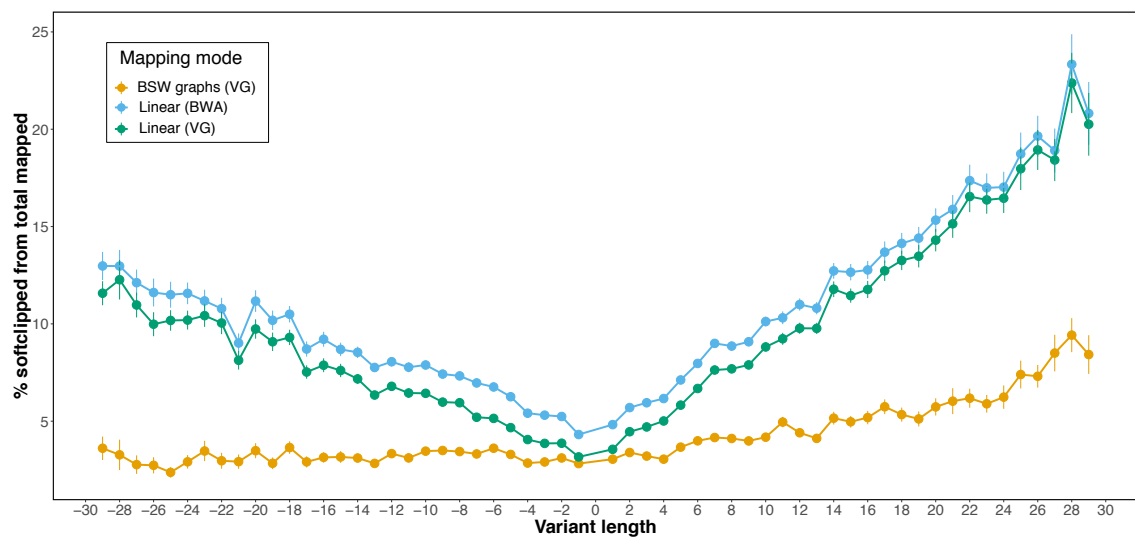
Figure S3.16: **Proportion of soft-clipped reads at heterozygous sites in graph (*vg*) and linear (*vg* and *BWA*) alignments.**
We considered only variants for which the alternate allele was already included in the graph. The circles represent the mean (± standard error of mean) values at a given variant length.

Truth (array)

Test (sequence)

	0/0	0/1	1/1
0/0			
0/1		■	■
1/1		■	■
./.			

Recall /
Non-reference Sensitivity

	0/0	0/1	1/1
0/0	■		
0/1		■	
1/1			■
./.			

Genotype
Concordance

	0/0	0/1	1/1
0/0			
0/1		■	
1/1			■
./.			

Non-reference discrepancy

	0/0	0/1	1/1
0/0			
0/1		■	
1/1			■
./.			

Precision
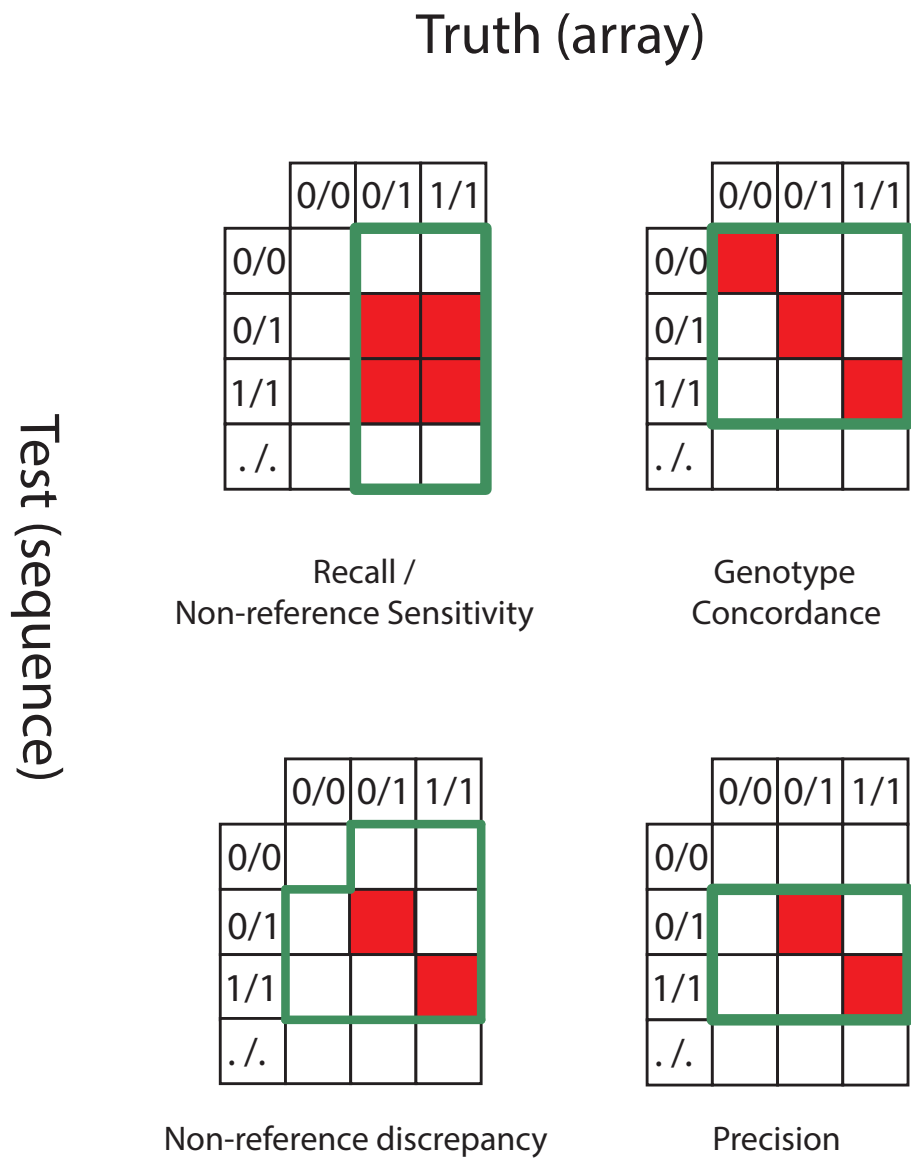
Figure S3.17: **Genotype concordance matrices for four quality parameters.** For each metric, we divided the sum of the red cells by the sum of the cells within the green frame.

Note S3.1

Comparison of variant prioritization approaches

We applied FORGe (Pritt et al., 2018) to prioritize variants to be added to the Brown Swiss reference graph for chromosome 25. Specifically, we considered the four variant ranking approaches implemented in FORGe and compared the mapping accuracy from the resulting graphs with a graph that was constructed with variants selected based on an allele frequency threshold.

The following prioritization approaches were investigated:

1. Pop Cov: variants ranked based on allele frequency

2. Pop Cov + blowup: variants ranked based on allele frequency and proximity (variants that are nearby receive lower scores)

3. Hybrid: variants ranked based on allele frequency and how the variants affect the resulting k-mer profile of the genome graph (variants that would increase the repetiveness of the resulting graph receive lower scores)

4. Hybrid + blowup: hybrid methods + considering variant proximity

5. AF threshold: variants ranked based on allele frequency (AF, as applied in our paper).

We refer to the FORGe paper (Pritt et al., 2018) for a detailed description on the implementation of the variant prioritization methods 1-4. For each prioritization approach, we constructed a number of graphs that included the top x% of the ranked variants, where x ranged from 1 to 100 with steps of 10 (e.g., a graph constructed with x=10 included 34,715 out of 347,147 bta25 Brown Swiss variants). We then mapped paired-end reads simulated form a Brown Swiss animal (as detailed in the Material and Methods part of the main manuscript) to the graphs in order to calculate mapping accuracy.

Graphs constructed with variants that were prioritized solely using allele frequency (as applied in our current paper and the Pop Cov method of FORGe) enable the most accurate mapping of reads (Table SN31 and Figure SN31). Considering additional factors other than allele frequency did not lead to further accuracy improvements. The mapping accuracy of the Pop Cov and AF threshold strategies was virtually identical when the same number of variants was used. The most accurate Pop Cov approach corresponds to an alternate allele frequency threshold of 0.06.

Table SN31: Comparison of the most accurate graph from each ranking method

Ranking methods	Minimum mapping error	Number of variants in the graphs with maximum accuracy
PopCov	0.0722	208288
PopCov + blowup	0.0730	208288
Variant frequency	0.0723	208288
Hybrid	0.0749	347147
Hybrid + blowup	0.0749	347147
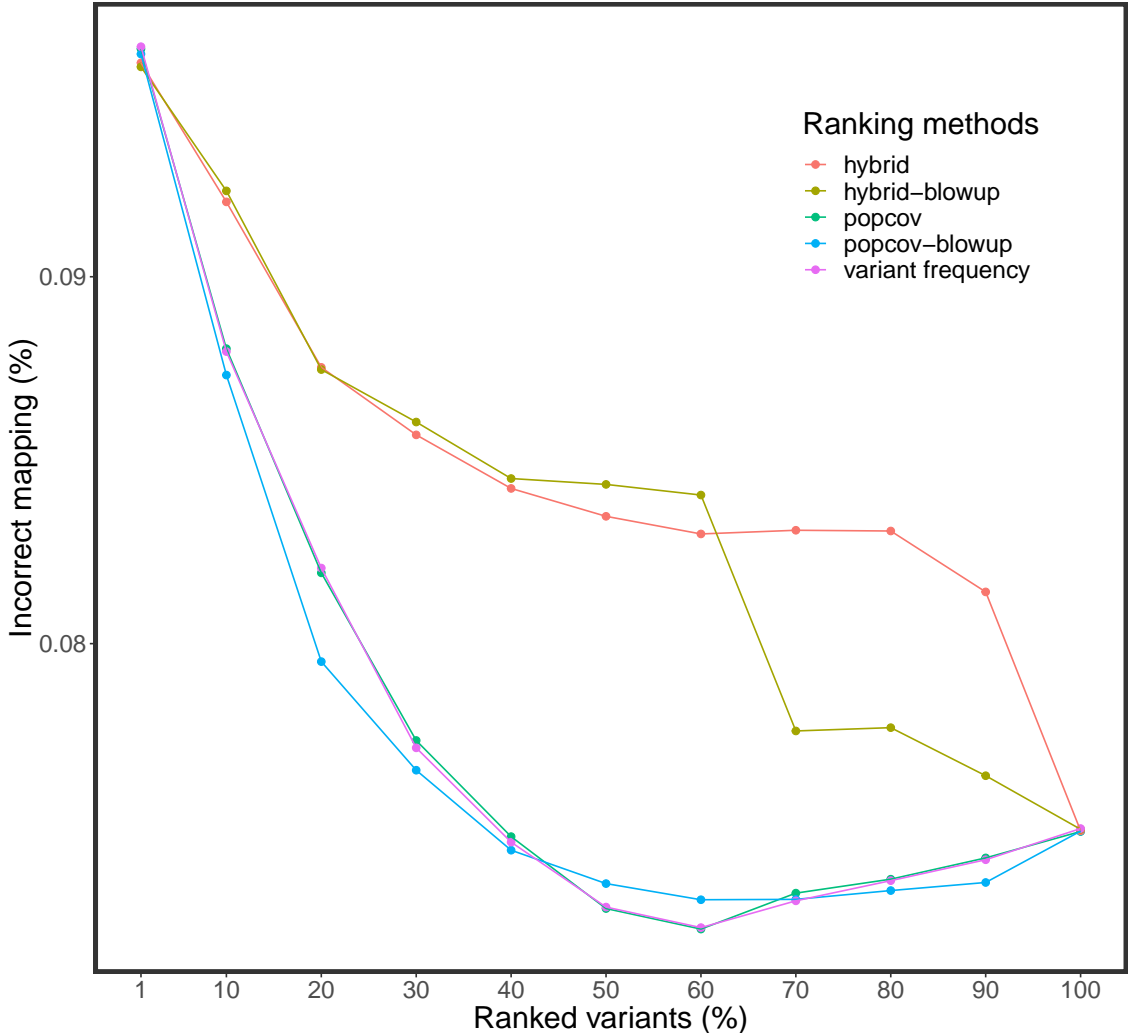
Figure SN31: Comparison of different variant prioritization strategies.
Proportion of incorrectly mapped reads for graphs constructed with five variant prioritization approaches.

Note S3.2

Adjusted (tuned) linear mapping approach

We followed the proposed approach outlined by (Grytten et al., 2020) to adjust the default parameters of *BWA mem* in order to also consider sub-optimal alignments. First, we reduce the D value (default 0.5) to consider more alternative alignment positions. However, the mapping performance changed only marginally.

Second, we ran *Minimap2* in short read mode (-ax sr) to find all suboptimal alignments. Subsequently, we retained for each read the read placement from either *BWA mem* or *Minimap2* that had the higher alignment score. For reads that had identical alignment score and position for both linear mappers, we retained the lower mapping quality score. For all other cases, we retained the *BWA mem* alignment.

We made two observations (Figure SN32):

1. The overall mapping accuracy increased mainly due to a smaller number of incorrectly placed reads that had high mapping quality (MQ > 10). This indicates that the tuned linear mapping approach assigns the quality of the alignments better.

2. We found an improvement in mapping accuracy only on reads that are identical to the reference, but not on reads that contain variants.

While Grytten et al. observed that an adjusted parameter setting of *BWA mem* and subsequent application of *Minimap2* led to considerable accuracy improvements, the gain in accuracy was low in our study. The proportion of simulated reads with variants was twice as high (19.16% vs. 10.6%) in our study than in Grytten et al., because the average number of polymorphic sites per genome was almost two-fold higher in cattle than humans.
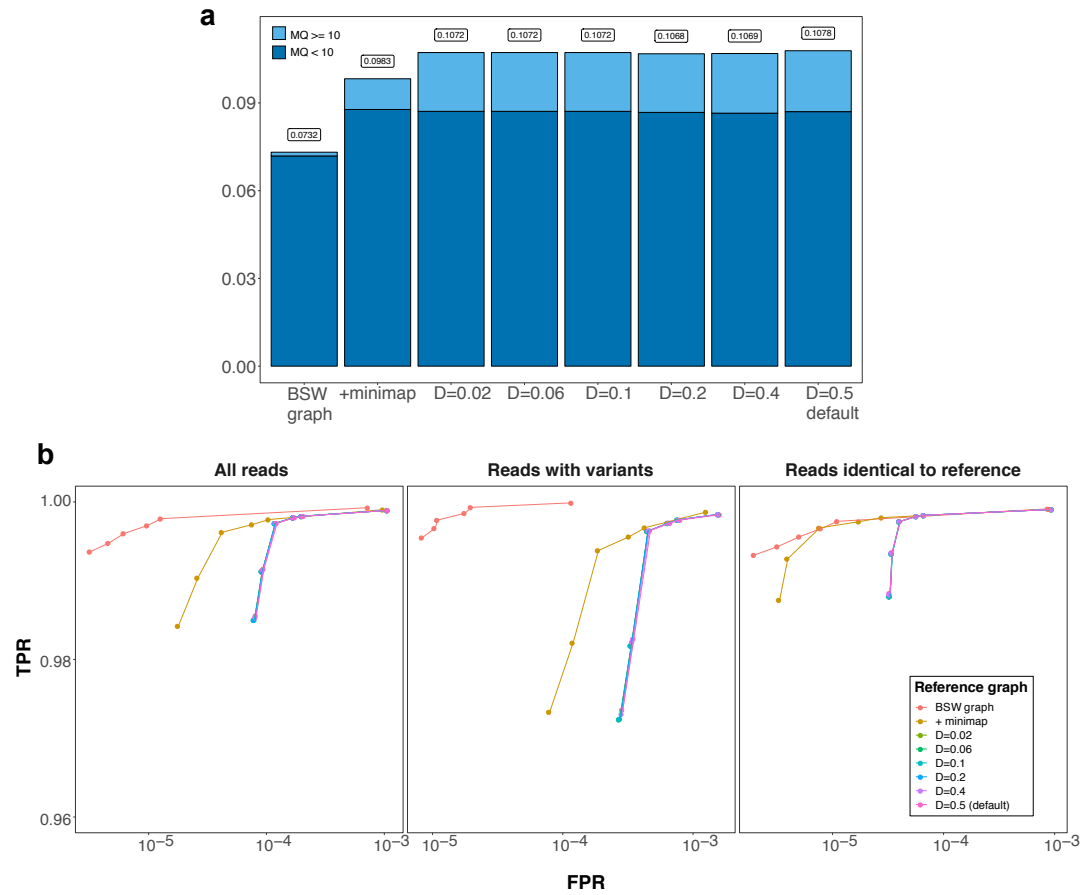
Figure SN32: Mapping accuracy of paired-end reads simulated form a Brown Swiss animal using different mapping approaches.
(a) Proportion of simulated reads with mapping errors for different mapping scenarios. (b) True positive and false positive rate parameterized on mapping quality for the different scenarios.

Note S3.3

Integrating structural variants into the graphs

We investigated the effect of including longer (structural) variants. For this purpose, we first called and genotyped structural variants using *Delly* (Rausch et al., 2012) from 82 Brown Swiss samples that had been sequenced using short-reads (see Material and Methods part of the main manuscript). We discovered 157 precise SVs on bovine chromosome 25 that had an average length of 178 bp. We then combined these variants with 243,145 SNPs and Indels that were discovered using *GATK*. We used the bta25 ARS-UCD1.2 reference as a backbone and constructed four graphs: (i) SNPs (+Indels) from *GATK*, (i) SVs from *Delly*, (iii) SNPs (+Indels) from *GATK* + SVs from *Delly*, (iv) empty (only the backbone, no variants). We simulated 10 million paired end reads from haplotypes of one Brown Swiss animal (SAMEA6272105, that had 121,996 SNPs + Indels and 57 SVs that were included in the graph). The simulated reads were mapped to the different graphs using *vg*.

Table SN32: Mapping accuracy for graphs that contained different variant types
MQ=0 and MQ < 10 indicates the proportion of reads mapped with mapping quality 0 and less than 10, respectively.

Graphs	Variants in the graphs	MQ=0 (%)	MQ<10 (%)	Mapping error (%)
Linear	0	0.15474	0.22310	0.08599
SNP	243,145	0.15366	0.21804	0.07995
SV	157	0.15508	0.22390	0.08629
SNP + SV	243,145 + 157	0.15458	0.21900	0.08003

Adding SVs that were detect from short sequencing reads to the graph marginally affected the mapping performance. Actually, the mapping accuracy decreased slightly when SVs were added. Read mapping accuracy improvements were attributable to the SNPs and Indels detected using *GATK*.

Table S3.1: **Properties of autosomal variants detected in human (JPT, GBR, STU, YRI) and bovine (HOL, FV, BSW, OBV) populations**

Species	Population	Number of samples	Variant count	Average per sample	Singleton variants	Variants with allele frequency < 0.05
Human	JPT	104	12,433,397	4,020,815	2,836,542 (22.81%)	5,580,288 (44.88%)
	GBR	91	13,148,448	4,011,102	2,878,144 (21.88 %)	6,005,303 (45.67%)
	STU	102	15,264,479	4,096,457	4,024,478 (26.34%)	7,915,678 (51.85%)
	YRI	108	22,420,039	4,863,955	4,702,120 (20.97%)	12,431,887 (55.45%)
Cattle	HOL	49	16,762,842	6,841,965	1,713,642 (10.22%)	3,964,699 (23.65%)
	FV	49	18,638,951	6,955,100	2,272,546 (12.19%)	5,112,547 (27.42%)
	BSW	82	20,446,693	6,983,517	3,957,703 (19.35%)	7,913,226 (38.70%)
	OBV	104	21,875,164	7,111,562	3,124,950 (14.28%)	8,250,961 (37.71%)

Table S3.2: **Properties of variants detected on human chromosome 19 and bovine chromosome 25 in human (JPT, GBR, STU, YRI) and bovine (HOL, FV, BSW, OBV) populations**

Species	Population	Number of samples	Variant count	Average per sample	Singleton variants	Variants with allele frequency < 0.05
Human	JPT	104	291,303	88,945	66,944 (22.98%)	135,289 (46.44%)
	GBR	91	306,304	90,988	64,119 (20.93 %)	138,076 (45.07%)
	STU	102	355,107	94,253	93,116 (26.22%)	181,300 (51.05%)
	YRI	108	521,021	118,429	106,734 (20.49%)	280,960 (53.92%)
Cattle	HOL	49	295,801	121,114	30,543 (10.32%)	67827 (22.92%)
	FV	49	336,390	125,597	43,783 (13.01%)	94,577 (28.11%)
	BSW	82	347,402	124,209	53,773 (15.47%)	128,990 (37.12%)
	OBV	104	387,855	126,158	47,498 (12.24%)	144,958 (37.37%)

Table S3.3: **Concordance between array-called and sequence variant genotypes that were discovered from either graph or linear alignments using _Samtools_, _GATK_, or _Graphtyper_.**

Numbers represent average values (± standard deviation) of 10 BSW animals for the raw (Full) and hard-filtered (Filtered) genotypes.

	Full			Filtered		
Samtools						
	Graph	Linear	Linear	Graph	Linear	Linear
	VG	VG	BWA	VG	VG	BWA
Genotype concordance	98.50(1.07)	98.47(1.07)	98.53(1.03)	98.53(1.07)	98.50(1.07)	98.55(1.04)
NR-sensitivity (Recall)	98.53(0.37)	98.52(0.39)	98.53(0.39)	97.48(0.36)	97.45(0.35)	97.53(0.36)
NR-discrepancy	2.21(1.60)	2.24(1.60)	2.17(1.55)	2.17(1.60)	2.20(1.61)	2.13(1.56)
Precision	98.90(0.83)	98.89(0.83)	98.93(0.81)	98.91(0.83)	98.90(0.83)	98.94(0.82)
GATK						
Genotype concordance	97.26(2.24)	97.24(2.25)	97.38(2.15)	97.26(2.25)	97.25(2.25)	97.39(2.15)
NR-sensitivity (Recall)	98.17(0.94)	98.16(0.94)	98.23(0.87)	98.14(0.94)	98.12(0.94)	98.18(0.87)
NR-discrepancy	4.09(3.38)	4.10(3.39)	3.89(3.23)	4.08(3.38)	4.09(3.39)	3.88(3.23)
Precision	98.90(0.83)	98.90(0.83)	98.94(0.80)	98.91(0.83)	98.91(0.83)	98.95(0.80)
Graphtyper						
Genotype concordance	98.57(1.01)	98.57(1.01)	98.61(0.97)	98.61(1.03)	98.61(1.03)	98.64(0.99)
NR-sensitivity (Recall)	98.34(0.54)	98.36(0.55)	98.37(0.53)	96.14(0.54)	96.13(0.54)	96.17(0.52)
NR-discrepancy	2.08(1.49)	2.08(1.50)	2.02(1.44)	2.01(1.50)	2.01(1.50)	1.97(1.45)
Precision	98.85(0.80)	98.84(0.81)	98.87(0.79)	98.89(0.82)	98.89(0.82)	98.91(0.80)

Table S3.4: **Accession numbers of the animals** used for variant detection, read simulation, sequence read mapping and genotyping

Accession	Breed	Graph construction	Simulation	Validation genotyping	Validation Mapping bias	Coverage
SAMEA4827645	OBV	x				14.41
SAMEA4827646	OBV	x				12.9
SAMEA4827647	OBV	x				14.79
SAMEA4827648	OBV	x				10.76
SAMEA4827649	OBV	x				11.55
SAMEA4827650	OBV	x				10.29
SAMEA4827651	OBV	x				14.76
SAMEA4827652	OBV	x				10.65
SAMEA4827653	OBV	x				9.69
SAMEA4827654	OBV	x				10.72
SAMEA4827655	OBV	x				11.32
SAMEA4827656	OBV	x				11.83
SAMEA4827657	OBV	x				8.47
SAMEA4827658	OBV	x				9.69
SAMEA4827659	OBV	x				9.52
SAMEA4827660	OBV	x				10.04
SAMEA4827661	OBV	x				9.68
SAMEA4827662	OBV	x				17.37
SAMEA4827663	OBV	x				11.2
SAMEA4827664	OBV	x				11.29
SAMEA4827665	OBV	x				13.07
SAMEA4827666	OBV	x				11.23
SAMEA4827667	OBV	x				10.99
SAMEA4827668	OBV	x				10.93
SAMEA4827669	OBV	x				12.89
SAMEA4827670	OBV	x				12.18
SAMEA4827671	OBV	x				11.35
SAMEA4827672	OBV	x				10.49
SAMEA4827673	OBV	x				10.31
SAMEA4827674	OBV	x				12.58
SAMEA5059741	OBV	x				4.58
SAMEA5059742	OBV	x				3.76
SAMEA5059743	OBV	x	x			22.33
SAMEA5059744	OBV	x				3.93
SAMEA5059745	OBV	x				4.31
SAMEA5059746	OBV	x				4.29
SAMEA5059747	OBV	x				4.58
SAMEA5059748	OBV	x				5.08
SAMEA5059749	OBV	x				5.19
SAMEA5059750	OBV	x				3.91
SAMEA5059751	OBV	x				5.59
SAMEA5059752	OBV	x				3.89
SAMEA5059753	OBV	x				4.18
SAMEA5059754	OBV	x				3.49
SAMEA5059755	OBV	x				7.49
SAMEA5059756	OBV	x				6.65
SAMEA5059757	OBV	x				5.74
SAMEA5059758	OBV	x				5.1

Accession	Breed	Graph construction	Simulation	Validation genotyping	Validation Mapping bias	Coverage
SAMEA6272117	OBV	x				6.43
SAMEA5059759	OBV	x				3.97
SAMEA5159792	BSW	x				10.68
SAMEA5159791	BSW	x				10.22
SAMEA5159788	BSW	x				10.71
SAMEA5159783	BSW	x				11.91
SAMEA5159785	BSW	x				11.94
SAMEA5159799	BSW	x				10.25
SAMEA5159787	BSW	x				13.63
SAMEA5159761	BSW	x				16.46
SAMEA5159782	BSW	x				11.47
SAMEA5159775	BSW	x				10.14
SAMEA5159786	BSW	x				12.04
SAMEA5159784	BSW	x				11.88
SAMEA5159798	BSW	x				12.79
SAMEA5159781	BSW	x				12.65
SAMEA5159780	BSW	x				12.41
SAMEA5159777	BSW	x				9.8
SAMEA5159797	BSW	x				11.98
SAMEA5159774	BSW	x				9.46
SAMEA5159769	BSW	x				12.3
SAMEA5159778	BSW	x				13.03
SAMEA5159771	BSW	x				10.92
SAMEA5159779	BSW	x				10.63
SAMEA5159772	BSW	x				11.88
SAMEA5159773	BSW	x				10.77
SAMEA5159793	BSW	x				12.6
SAMEA5159770	BSW	x				10.01
SAMEA5159795	OBV	x				12.58
SAMEA5159768	OBV	x				8.69
SAMEA5159796	OBV	x				11.39
SAMEA5159789	OBV	x				10.27
SAMEA5159790	OBV	x				10.52
SAMEA5159794	OBV	x				11.46
SAMEA5159776	OBV	x				9.71
SAMEA5159767	OBV	x				10.17
SAMN05216093	OBV	x				10.85
SAMN05216095	OBV	x				11.12
SAMN05216094	OBV	x				10.64
SAMN05216096	OBV	x				11.51
SAMEA6272131	FV	x				13.4
SAMEA6272130	FV	x				10.41
SAMEA4644727	BSW	x				14.86
SAMEA4644728	BSW	x				14.86
SAMEA19864918	BSW	x				9.23
SAMEA4644765	BSW	x				12.14
SAMEA4644766	BSW	x				16.48
SAMEA4644768	OBV	x				13.41
SAMEA4644769	BSW	x				16.04
SAMEA19312918	BSW	x				4.43

Continuation of Table S3.4

Accession	Breed	Graph construction	Simulation	Validation genotyping	Validation Mapping bias	Coverage
SAMEA19313668	BSW	x				7.13
SAMEA19314418	BSW	x				10.99
SAMEA19315168	BSW	x				9.7
SAMEA19318918	BSW	x				6.9
SAMEA19323418	BSW	x				18.83
SAMEA4644754	BSW	x				15.25
SAMEA4644755	BSW	x				13.58
SAMEA4644756	BSW	x				13.88
SAMEA4644730	OBV	x				14.85
SAMEA4644734	OBV	x				15.3
SAMEA4644735	BSW	x				9.43
SAMEA4644757	BSW	x				11.36
SAMEA4644739	BSW	x				14.13
SAMEA4644740	OBV	x				15.73
SAMEA4644741	BSW	x				15.57
SAMEA4644742	BSW	x				15.68
SAMEA4644758	BSW	x				13
SAMEA4644743	BSW	x				15.46
SAMEA4644749	OBV	x				13.85
SAMEA4644750	OBV	x				15.25
SAMEA4644762	BSW	x				13.92
SAMEA4644763	BSW	x				11.62
SAMEA4644764	OBV	x				10.57
SAMN07692225	BSW	x				10.72
SAMN02671625	FV	x				5.06
SAMN02671626	FV	x	x			23.24
SAMN02671627	FV	x				6.32
SAMN02671628	FV	x				4.95
SAMN02671629	FV	x				8.41
SAMN02671630	FV	x				4.88
SAMN02671631	FV	x				4.77
SAMN02671632	FV	x				7.64
SAMN02671633	FV	x				3.59
SAMN02671634	FV	x				7.67
SAMN02671635	FV	x				6.37
SAMN02671636	FV	x				6.26
SAMN02671637	FV	x				3.79
SAMN02671638	FV	x				3.95
SAMN02671639	FV	x				7.21
SAMN02671640	FV	x				8.62
SAMN02671641	FV	x				6.08
SAMN02671642	FV	x				5.47
SAMN02671643	FV	x				5.03
SAMN02671644	FV	x				4.35
SAMN02671645	FV	x				5.06
SAMN02671646	FV	x				5.79
SAMN02671647	FV	x				5.2
SAMN02671648	FV	x				5.81
SAMN02671649	FV	x				5.32
SAMN02671650	FV	x				5.34

Continuation of Table S3.4

Accession	Breed	Graph construction	Simulation	Validation genotyping	Validation Mapping bias	Coverage
SAMN02671651	FV	x				4.51
SAMN02671652	FV	x				7.48
SAMN02671653	FV	x				7.5
SAMN02671654	FV	x				7.6
SAMN02671655	FV	x				7.19
SAMN02671656	FV	x				5.4
SAMN02671657	FV	x				5.61
SAMN02671658	FV	x				4.91
SAMN02671659	FV	x				4.83
SAMN02671661	FV	x				5.58
SAMN02671662	FV	x				6.08
SAMN02671663	FV	x				5.06
SAMN02671664	FV	x				7.95
SAMN02671665	FV	x				6.53
SAMN02671666	FV	x				6.06
SAMN02671667	FV	x				8.13
SAMN02671572	HOL	x				6.79
SAMN02671574	HOL	x				10.25
SAMN02671576	HOL	x				5.02
SAMN02671578	HOL	x				19.78
SAMN02671580	HOL	x				10.52
SAMN02671582	HOL	x				15.22
SAMN02671584	HOL	x	x			29.97
SAMN02671586	HOL	x				17.21
SAMN02671588	HOL	x				16.99
SAMN02671590	HOL	x				13.79
SAMN02671592	HOL	x				16.31
SAMN02671594	HOL	x				19.56
SAMN02671596	HOL	x				16.43
SAMN02671455	HOL	x				9.23
SAMN02671457	HOL	x				10.28
SAMN02671459	HOL	x				8.4
SAMN02671461	HOL	x				9.47
SAMN02671463	HOL	x				6.36
SAMN02671465	HOL	x				10.61
SAMN02671467	HOL	x				9.78
SAMN02671469	HOL	x				9.13
SAMN02671471	HOL	x				6.49
SAMN02671473	HOL	x				8.71
SAMN02671475	HOL	x				9.57
SAMN02671477	HOL	x				10.89
SAMN02671479	HOL	x				8.81
SAMN02671481	HOL	x				8.59
SAMN02671483	HOL	x				10.79
SAMN02671485	HOL	x				9.18
SAMN02671487	HOL	x				10.1
SAMN02671489	HOL	x				10.06
SAMN02671491	HOL	x				9.83
SAMN02671493	HOL	x				10.1
SAMN02671495	HOL	x				8.58

Accession	Breed	Graph construction	Simulation	Validation genotyping	Validation Mapping bias	Coverage
SAMN02671613	HOL	x				23.58
SAMN02671615	HOL	x				20.36
SAMN02671617	HOL	x				20.36
SAMN02671619	HOL	x				12.54
SAMN02671621	HOL	x				12.86
SAMN02671623	HOL	x				4.73
SAMN02671668	HOL	x				11.92
SAMN02671670	HOL	x				11.35
SAMN02671672	HOL	x				10.21
SAMN02671674	HOL	x				10.4
SAMN02671676	HOL	x				11.21
SAMN02671725	HOL	x				11.54
SAMN02671727	HOL	x				5.43
SAMN02671729	HOL	x				13.68
SAMN02671731	HOL	x				13.58
SAMEA6272085	OBV	x				8.01
SAMEA6272091	OBV	x				9.55
SAMEA6272090	OBV	x				10.74
SAMEA6272089	OBV	x				8.25
SAMEA6272088	OBV	x				10.97
SAMEA6272093	OBV	x				11.3
SAMEA6272087	OBV	x				11.62
SAMEA6272086	OBV	x				12.58
SAMEA6272092	OBV	x				9.38
SAMEA6272094	OBV	x				8.31
SAMEA6272115	OBV	x				8.65
SAMEA6272114	OBV	x				8.06
SAMEA6272112	OBV	x				9.51
SAMEA6272113	OBV	x				10.61
SAMEA6272110	OBV	x				7.99
SAMEA6272103	OBV	x				9.09
SAMEA6272109	OBV	x				7.97
SAMEA6272107	OBV	x				10.34
SAMEA6272102	OBV	x				7.25
SAMEA6272100	OBV	x				8.55
SAMEA6272133	FV	x				12.73
SAMEA6272134	FV	x				10.25
SAMEA6272128	FV	x				11.09
SAMEA6163196	BSW	x				11.48
SAMEA6163197	BSW	x				9.86
SAMEA6163198	BSW	x				11.63
SAMEA6163199	BSW	x				13.68
SAMEA6272129	FV	x				14.9
SAMEA6272132	FV	x				15.25
SAMEA6272119	OBV	x				19.58
SAMEA6272123	OBV	x				16.93
SAMEA6272118	OBV	x				18.66
SAMEA6272120	OBV	x				18.5
SAMEA6272121	OBV	x				16.58
SAMEA6272126	OBV	x				61.9

Accession	Breed	Graph construction	Simulation	Validation genotyping	Validation Mapping bias	Coverage
SAMEA6272124	OBV	x				18.82
SAMEA6272122	OBV	x				18.33
SAMEA6272127	OBV	x				53.65
SAMEA6272125	OBV	x				23.01
SAMEA6272084	OBV	x				11.78
SAMEA6272083	OBV	x				31.95
SAMEA6272082	OBV	x				23.39
SAMEA6272095	BSW	x				25.36
SAMEA6272096	BSW	x				20.6
SAMEA6272097	BSW	x				10.68
SAMEA6272098	BSW	x				15.25
SAMEA6272099	BSW	x				12.32
SAMEA6272101	BSW	x				10.4
SAMEA6272104	BSW	x				12.63
SAMEA6272105	BSW	x	x			33.7
SAMEA6272106	BSW	x				15.76
SAMEA6272108	BSW	x				20.46
SAMEA6272111	BSW	x				28.82
SAMEA6272116	BSW	x				70.04
SAMEA5159861	BSW	x				24.84
SAMEA5159863	BSW	x				23.64
SAMEA5159864	BSW	x				24.92
SAMEA5159865	BSW	x				25.99
SAMEA5159866	BSW	x				25.11
SAMEA5159867	BSW	x				26.28
SAMEA5159868	BSW	x				26.73
SAMEA5159869	BSW	x				27.62
SAMEA5159870	BSW	x				32.64
SAMEA5159871	BSW	x				34.49
SAMEA5159872	BSW	x				27.96
SAMEA5159873	BSW	x				24.08
SAMEA5159874	BSW	x				33.8
SAMEA5159875	BSW	x				22.66
SAMEA5159885	BSW	x				23.1
SAMEA5159837	OBV	x				28.12
SAMEA5159843	OBV	x				22.81
SAMEA5159848	OBV	x				22.5
SAMEA5159849	OBV	x				26.32
SAMEA5159850	OBV	x				27.69
SAMEA5159886	OBV	x				35.51
SAMEA6163185	BSW			x	x	39.88
SAMEA6163188	BSW			x		25.74
SAMEA6163187	BSW			x		20.29
SAMEA6163177	BSW			x		8.26
SAMEA6163178	BSW			x		5.74
SAMEA6163176	BSW			x		9.29
SAMEA6163179	BSW			x		6.93
SAMEA6163183	BSW			x		7.86
SAMEA6163181	BSW			x		7.97
SAMEA6163182	BSW			x		8.36

Supplementary References

W. Beyer, A. M. Novak, G. Hickey, J. Chan, V. Tan, B. Paten, and D. R. Zerbino. Sequence tube maps: making graph genomes intuitive to commuters. *Bioinformatics*, 35(24):5318, 2019.

I. Grytten, K. D. Rand, A. J. Nederbragt, and G. K. Sandve. Assessing graph-based read mappers against a baseline approach highlights strengths and weaknesses of current methods. *BMC genomics*, 21:1–9, 2020.

J. Pritt, N.-C. Chen, and B. Langmead. Forge: prioritizing variants for graph genomes. *Genome biology*, 19(1):1–16, 2018.

T. Rausch, T. Zichner, A. Schlattl, A. M. Stütz, V. Benes, and J. O. Korbel. Delly: structural variant discovery by integrated paired-end and split-read analysis. *Bioinformatics*, 28(18):i333–i339, 2012.